Impact of static and dynamic deformations in the decay of ^{197}Tl* compound nucleus

Gayatri Sarkar[1], Amandeep Kaur[2], Moumita Maiti[1],* and Manoj K. Sharma[2]
[1] *Department of Physics, Indian Institute of Technology Roorkee, Roorkee-247667, INDIA and*
[2] *School of Physics and Materials Science, Thapar Institute of Engineering and Technology, Patiala-147004, INDIA*

Introduction

A comprehensive information on the collective motion of nuclear systems may be acquired by measuring the properties of evaporated residue (ER) and fusion-fission (ff) fragments. Several efforts have been undertaken to get an insight of the decay dynamics of compound nuclei (CNs) in the mass region of A≈200, as elements of this region play an important role in synthesis of super-heavy elements. In view of this, a theoretical attempt has been made in the framework of dynamical cluster-decay model (DCM) [1] to explore the decay patterns of ^{197}Tl* formed via ^{16}O+^{181}Ta reaction at excitation energy, E^*_{CN}=45 MeV. The calculations are done using spherical and quadrupole (β_2) deformed decay fragments with optimum orientations of hot-compact and cold-elongated configurations. Moreover, the relative analysis of static (T-independent) and dynamic (T-dependent) deformations is also carried out to investigate the distribution pattern of fission fragments.

Methodology

DCM works in terms of the collective coordinates such as mass asymmetry parameter (η_A), relative separation R between two fragments, multipole deformations $\beta_{\lambda i}$ and orientations θ_i (where, $i = 1, 2$ for heavy and light fragment). The deformation parameters are also made temperature dependent, by using the relation: $\beta_{\lambda i}(T) = exp(-T/T_0)\beta_{\lambda i}(0)$, where $\beta_{\lambda i}(0)$ represents the static deformation and T_0 is the temperature of the nucleus at which shell effects start to vanish (T_0 = 1.5 MeV). Using these coordinates, the fragmentation potential $V(\eta, T)$ is calculated at a fixed R as, $V(\eta, T) = -\sum_{i=1}^{2}[B_i(A_i, Z_i, T)] + V_C + V_P + V_\ell$. B_i, V_C, V_P and V_ℓ are, respectively, the binding energy, Coulomb interaction, nuclear proximity and centrifugal potentials [1]. $V(\eta, T)$ is further used as an input in Schrödinger equation of η-coordinate to obtain preformation probability P_0 of decaying fragments as: $P_0 = |\psi[\eta(A_i)]|^2 \frac{2}{A_{CN}}\sqrt{B_{\eta\eta}}$. $B_{\eta\eta}$ are the smooth hydrodynamical mass parameters. The CN decay cross section are calculated using ℓ partial waves method. For more details see [1].

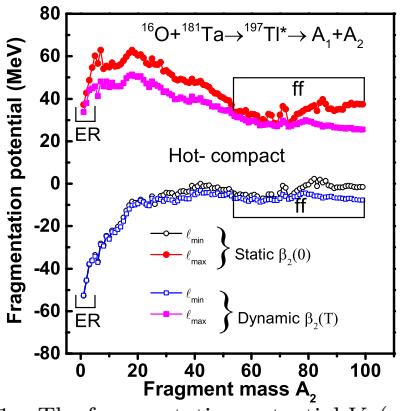

FIG. 1: The fragmentation potential $V_R(\eta, T)$ as a function of A_2 for the decay of ^{197}Tl* nucleus.

Results and discussion

Fig. 1 represents the fragmentation potential as a function of fragment mass A_2 for the decay of ^{197}Tl* nucleus at E^*_{CN}=45 MeV ($E_{c.m.}$=69.94 MeV) by incorporating static ($\beta_{\lambda i}(0)$) and dynamic ($\beta_{\lambda i}(T)$) quadrupole deformations with hot-compact orientations at ℓ_{min}=20$\hbar$ and ℓ_{max}=124$\hbar$ values. A careful look at the fragmentation plot suggests that the structure and magnitude of fragmentation

*Electronic address: moumita.maiti@ph.iitr.ac.in

TABLE I: DCM calculated ERs cross section using spherical, β_2 (static & dynamic) deformations.

$E_{c.m.}$	Spherical		β_2-Static				β_2-Dynamic				
			Hot		Cold		Hot		Cold		
	ΔR	σ	ΔR	σ	ΔR	σ	ΔR	σ	ΔR	σ	$\sigma_{Expt.}$
(MeV)	(fm)	(mb)	(fm)	(mb)	(fm)	(mb)	(fm)	(mb)	(fm)	(mb)	(mb)
69.64	1.69	101.0	1.64	107.9	2.14	101.0	1.68	107.4	1.74	101.1	101.05

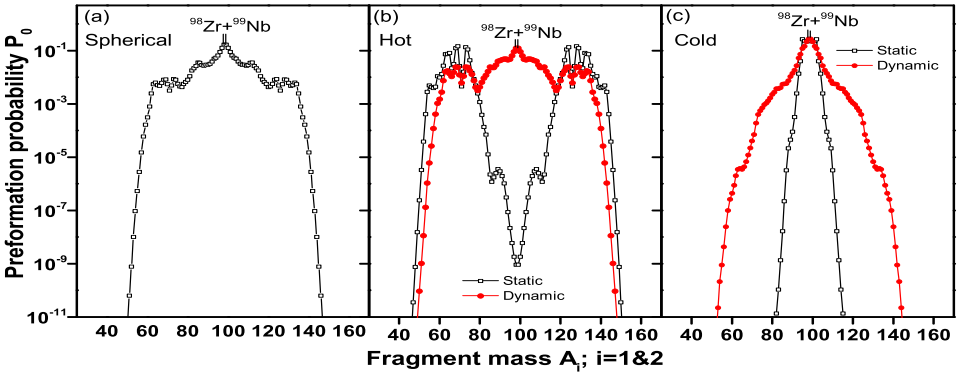

FIG. 2: Preformation probability P_0 as a function of fragment mass for the decay of ^{197}Tl* using (a) spherical, (b) β_2-deformed (static & dynamic) hot-compact, and (c) cold-elongated configurations.

potential are modified with temperature effects in the deformation parameter. Moreover, the minimum value of ℓ is more prone to the decay of light particles, and the emission of fission fragments at higher ℓ values takes place. Table I represents the DCM-calculated evaporation residue cross-sections along with other parameters for all considered approaches. The calculated cross-sections show nice agreement with the experimental data [2]. Note that fission cross-section data is not available at considered energy. Further, to see the effect of dynamic deformations in the fission region, the preformation probability P_0 of ^{197}Tl* is plotted at ℓ_{max}=124$\hbar$ in Figs. 2(a,b,c) for three configurations such as spherical, hot-compact and cold-elongated. A broad symmetric peak is observed in Fig. 2(a) for the case of the spherical approach. Fig. 2(b) represents an asymmetric fission distribution for the case of static deformations. After including dynamic deformations, the asymmetric behaviour of hot-compact configurations changes to triple humped mass distribution but having a higher probability of symmetric fission. For the case of the cold-elongated approach in Fig. 2(c), the sharp symmetric fission peak broadens with the inclusion of dynamic deformations. Overall, one can say that the symmetric fission pattern is observed for the spherical and dynamic deformed approach of both hot and cold orientations. This symmetric division of the nucleus is in agreement with the experimental result of Ref. [3]. Moreover, the choice of most probable symmetric fragments (i.e., ^{98}Zr+^{99}Nb) remain the same, independent of the choice of fragment orientations for β_2-dynamic case.

Acknowledgement

Research Grant No. INT/RUS/RFBR/387 from DST(IN) and fellowship from MHRD are gratefully acknowledged by M.M and G.S., respectively.

References

[1] R. K. Gupta *et. al*, Phys. Rev. C **70**, 034608 (2004).
[2] P. Jisha *et. al*, Phys. Rev. C **101**, 024611 (2020).
[3] V. R. Sharma *et. al*, Phys. Rev. C **84**, 014612 (2011).